Oxygen Vacancy Origin of the Surface Band-Gap State of TiO$_2$(110)

C. M. Yim, C. L. Pang, and G. Thornton

London Centre for Nanotechnology and Department of Chemistry, University College London,
17-19 Gordon Street, London WC1H 0AH, United Kingdom
(Received 13 November 2009; published 22 January 2010)

Scanning tunneling microscopy and photoemission spectroscopy have been used to determine the origin of the band-gap state in rutile TiO$_2$(110). This state has long been attributed to oxygen vacancies (O$_b$ vac). However, recently an alternative origin has been suggested, namely, subsurface interstitial Ti species. Here, we use electron bombardment to vary the O$_b$ vac density while monitoring the band-gap state with photoemission spectroscopy. Our results show that O$_b$ vac make the dominant contribution to the photoemission peak and that its magnitude is directly proportional to the O$_b$ vac density.

Metal oxides play an important role in a number of technologies such as catalysis, light-harvesting, and gas sensing [1]. Surface oxygen vacancies have long been thought to dominate the reactivity of oxide surfaces and therefore much research is directed towards understanding such defects. Rutile titania, particularly its most stable (110) face, has been used extensively as a model substrate to explore the surface physics and chemistry of metal oxides in general [2,3].

The TiO$_2$(110) surface is composed of alternating [001]-direction rows of fivefold coordinated Ti^{4+} ions (Ti$_{5c}$) and twofold coordinated bridging O^{2-} ions (O$_b$). Rutile TiO$_2$ is a wide band-gap insulator ($\sim$3 eV) which can be made semiconducting upon reduction by ion sputtering and annealing. This sample preparation results in the creation of oxygen vacancies, including bridging O vacancies (O$_b$ vac) at the surface (as shown in Fig. 1), and interstitial Ti species [2,4,5]. For such surfaces, a band-gap state is found about 1 eV below the Fermi level (E_F) in ultraviolet photoemission spectroscopy (UPS) [6,7] and as a $\sim$1 eV loss in electron energy loss spectroscopy (EELS) [8]. This state has been determined to have Ti $3d$ character by resonant photoemission studies [7,9].

Exposing the surface to O$_2$ eliminates the band-gap state so it was concluded that the state originates from O$_b$ vac that are themselves filled by oxygen atoms upon exposure to O$_2$ [7]. Thus, when O$_b$ vac are formed on the TiO$_2$(110) surface, two excess electrons associated with each O$_b$ vac are thought to transfer to the empty $3d$ orbitals of the neighboring Ti$_{5c}$ ions, forming two Ti^{3+} sites [6]. This picture, proposed by Henrich and co-workers based on the creation of band-gap states by Ar-ion bombardment [6], is known as the O-vacancy model.

Water is also known to fill the O$_b$ vac on TiO$_2$(110) from a temperature above 187 K [3], in this case replacing them with two hydroxyl species (OH$_b$) [10–12]. However, exposing the surface to water does not have a substantial effect on the magnitude of the band-gap state [7,13]. Hence, under the O-vacancy model, the band-gap state

should be present when either O$_b$ vac *or* OH$_b$ are present at the surface.

While this O-vacancy model has been widely accepted, Wendt *et al.* [14] recently proposed an intriguing alternative origin of the band-gap state. They found that when dosing O$_2$ onto a hydroxylated TiO$_2$(110) surface, the OH$_b$ were apparently eliminated but the band-gap state still persisted. From this, it was concluded that O$_b$ vac cannot be the main origin of the band-gap state. Instead it was suggested that interstitial Ti atoms make the dominant contribution to the band-gap state. Accompanying density functional theory (DFT) calculations indicate that interstitial Ti can indeed lead to band-gap states and that O$_b$ vac do not lead to such states.

Overall, however, the theoretical picture regarding the origin of the band-gap state is not clear: a number of calculations do predict that O$_b$ vac should lead to the formation of the band-gap state observed in photoemission [15–17], while a recent spin-polarized hybrid DFT calculation also suggests that Ti^{3+} interstitials can contribute to the band-gap state [18].
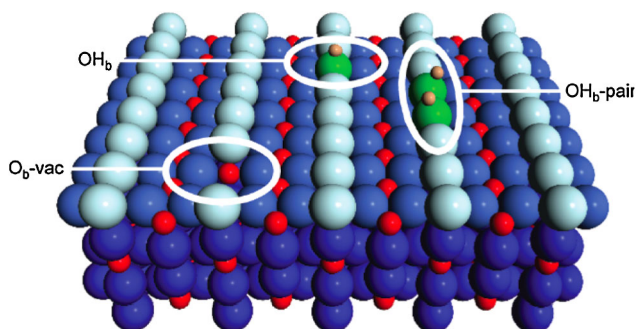

FIG. 1 (color online). A ball model of TiO$_2$(110). Small, red spheres denote fivefold coordinated Ti (Ti$_{5c}$) ions. Large, blue spheres represent O ions with twofold coordinated bridging O atoms shaded lighter. An oxygen vacancy (O$_b$ vac), an individual hydroxyl (OH$_b$), and a pair of hydroxyl species (OH$_b$ pair) are shown.

In this Letter, we resolve this issue experimentally by monitoring the band-gap state as a function of the O_b vac density. The O_b vac concentration was varied by bombarding the $TiO_2(110)$ surface with low energy electrons [19]. By preparing the surface in this way rather than by thermal annealing, the number of interstitial Ti in the near-surface region is kept constant [20]. The O_b vac concentration is determined from STM analysis of the surface before and after the UPS measurement, which is carried out in the same instrument. Our results show that there is a direct correlation between the concentration of O_b vac and the intensity of the photoemission band-gap state, thus providing direct evidence for the oxygen vacancy model.

The STM measurements were performed at ~ 78 K in a bath cryostat *Omicron* STM housed in an ultrahigh vacuum chamber with a base pressure of 2×10^{-11} mbar. The He I ($h\nu = 21.2$ eV) UPS data were measured in an adjoining preparation chamber (base pressure of 1×10^{-10} mbar) with a VSW HA125 hemispherical energy analyzer and a five-channel electron multiplier array. Normal emission UPS spectra were recorded at an incidence angle of 45° with respect to the surface normal. E_F was determined from the tantalum sample holder which was in electrical contact with the sample. The preparation chamber was also equipped with facilities for x-ray photoemission spectroscopy and low energy electron diffraction, which were used to confirm the sample cleanliness and long-range order.

Samples were prepared initially by cycles of Ar-ion sputtering and annealing to ~ 1000 K. Electron bombardment experiments employed a negatively biased filament (75 eV) with the sample grounded [19]. To minimize water contamination from the residual vacuum during the UPS measurement, the sample was held at ~ 500 K which prevents water adsorption [4]. We checked that holding the substrate at this temperature does not affect the O_b vac density, as measured by STM, or change the magnitude of the UPS band-gap state peak. Static secondary ion mass spectroscopy shows that the Ti:O ratio in the selvedge is essentially invariant between 400 and 700 K [5]. Hence, the concentration of interstitial Ti will not change over the course of the UPS measurements.

Figure 2(a) shows the STM image of an as-prepared $TiO_2(110)$ surface (r-TiO_2) collected using a light blue TiO_2 crystal (the color indicating a lightly reduced crystal [21]). The bright rows in the STM image arise from Ti_{5c} rows whereas the dark rows correspond to O_b rows [2]. Point defects such as O_b vac and single and paired surface hydroxyls (OH_b) appear as bright spots between the bright rows, O_b vac being slightly darker than OH_b, which are themselves darker than OH_b pairs. $TiO_2(110)$ almost always contains surface hydroxyls formed by water dissociation at O_b vac sites. Hence, when counting the number of O_b vac present at the surface, we also count every two isolated OH_b as a single O_b vac and every OH_b-pair as a single O_b vac [10,12]. In this way, we have calculated the *initial* density of O_b vac on the as-prepared surface to be $4.3 \pm 0.6\%$ ML, where 1 ML (monolayer) is defined as the
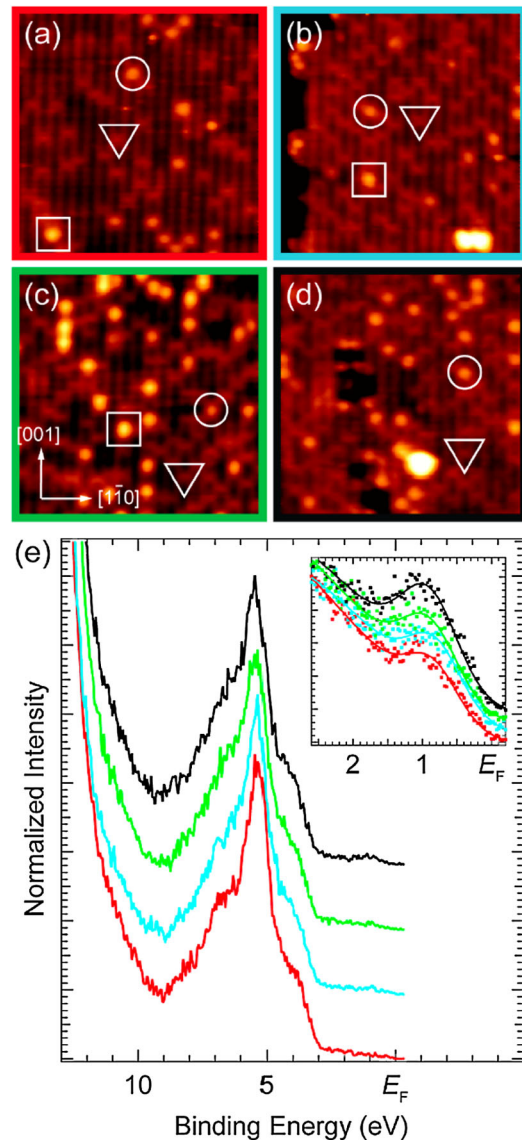

FIG. 2 (color online).   STM images (125×125 Å^2) of (a) the as-prepared $TiO_2(110)$ surface (r-TiO_2) and its appearance following electron bombardment (kinetic energy ~ 75 eV, ~ 1 mA) for (b) 5, (c) 10, and (d) 20 s. Symbols indicate O vacancies (triangles), bridging hydroxyls (circles), and hydroxyl pairs (squares). STM images were collected with a tunneling current ≤ 0.2 nA and a sample bias voltage of 1.3 V. (e) Corresponding UPS He I spectra of as-prepared r-TiO_2 (red) and after electron bombardment for 5 (light blue), 10 (green), and 20 s (black), all recorded under identical conditions. The inset in (e) shows the band-gap state region in more detail. The data points are shown as squares and the curves are the best fit to a Gaussian and polynomial background. The spectra are vertically offset for clarity. The spectra in (e) corresponding to each surface are color-coded with the color borders in (a)–(d). STM images and UPS spectra were collected at ~ 78 and ~ 500 K, respectively.

density of (1×1) unit cells, 5.2×10^{14} cm^{-2}. The coverage here, and throughout this study, was determined from five separate 250×250 Å^2 STM images collected from macroscopically different parts of the surface.

Figures 2(b)–2(d) show the STM images of the r-TiO$_2$ surface after it was bombarded with 75 eV electrons for different durations. The current density at the surface was estimated to be ~0.2 mA/cm^2. After electron bombardment, the O$_b$ vac density increases. The densities of O$_b$ vac on the TiO$_2$ surfaces after electron bombardment are 8.0 ± 0.2% ML for 5 s, 9.6 ± 0.5% ML for 10 s, and 9.2 ± 0.2% ML for 20 s. It should be noted that the surfaces following electron bombardment for 10 and 20 s have similar O$_b$ vac densities. However, the surface that has been exposed for 20 s is also decorated with pitlike features [19]. These features have a density of 0.15 ± 0.06% ML, about 100 times lower than the O$_b$ vac density and we assume they do not have a substantial effect on the band-gap state.

UPS was employed to monitor the band-gap state during the experiment. Figure 2(e) shows spectra corresponding to r-TiO$_2$ before and after electron bombardment. The spectrum of r-TiO$_2$ (red) is similar to that reported previously [22]. The main peak at ~5.5 eV and the shoulder at ~7.0 eV below E_F are mainly O 2p derived [22]. Electron bombardment causes the O 2p band to shift away from E_F due to band-bending, with the extent of the shift increasing with the duration of electron bombardment. The inset of Fig. 2(e) shows the UPS spectra measured across the band-gap state region (from 2.5 eV to E_F). The Ti 3d derived band-gap state (located ~0.9 eV below E_F) is clearly present in the spectrum of r-TiO$_2$. The intensity of this peak also clearly increases following electron bombardment.

We also collected data on an as-prepared surface of a dark blue TiO$_2$(110) crystal, the dark blue color indicating a more reduced crystal [21]. The STM image in Fig. 3(b) shows that the surface from the dark blue crystal contains a greater density of O$_b$ vac than the light blue sample, as one would expect. The O$_b$ vac density on the dark blue crystal is 6.7 ± 0.8% ML compared to 4.3 ± 0.6% ML for the light blue sample. As for UPS, the spectrum recorded from the dark blue crystal has a more intense band-gap state peak than in the case of the light blue sample. The area of the band-gap state peak for both samples, including the electron bombarded surfaces, is plotted against the O$_b$ vac density in Fig. 4(a). The graph fits easily to a straight line, clearly indicating that the peak area is in direct proportion to the O$_b$ vac density. Thus it is clear that the population of the band-gap state depends directly on the concentration of O$_b$ vac.

As we have already discussed above, O$_b$ vac on r-TiO$_2$ react with water molecules above 187 K [3], forming two OH$_b$ for each O$_b$ vac site. The OH$_b$ density is therefore highly correlated with the underlying O$_b$ vac density but does not have any direct relationship with the interstitial Ti density. Thus, if the band-gap state originates from O$_b$ vac, then the intensity of the peak in UPS should scale with the OH$_b$ density as well as the O$_b$ vac density.

Figure 4(b) summarizes a series of experiments performed on an initially hydroxylated surface of the dark
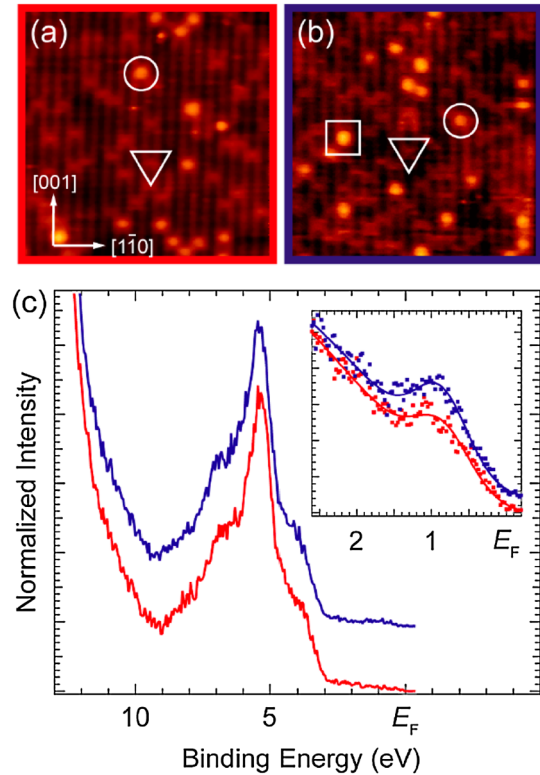

FIG. 3 (color online).   STM images (125 × 125 Å^2) of the as-prepared TiO$_2$(110) surface (r-TiO$_2$) of (a) a less-reduced (light blue) and (b) a more-reduced (dark blue) sample, collected with a tunneling current ≤ 0.2 nA and a sample bias voltage of 1.3 V. Symbols indicate O$_b$ vac (triangles), OH$_b$ (circles), and a OH$_b$ pair (square). (c) Corresponding UPS He I spectra taken on the less-reduced (red spectrum) and more-reduced (blue spectrum) TiO$_2$(110) surface. The inset shows the band-gap state region in more detail, with the more-reduced surface exhibiting a larger band-gap state peak in the spectra. The data points are shown as squares and the curves are the best fit to a Gaussian and polynomial background. The spectra are vertically offset for clarity. The spectra in (c) corresponding to each surface are color coded with the color borders in (a)–(b).

blue sample TiO$_2$(110) crystal. Like Fig. 4(a), it shows a graph of the intensity of the band-gap state peak in UPS plotted against the initial O$_b$ vac concentration (which is calculated by considering that every two OH$_b$ species originates from one initial O$_b$ vac). The data point marked with a filled square represents the initially hydroxylated surface. This surface was exposed to 10 Langmuirs (L) of O$_2$ at room temperature, where 1 L corresponds to an exposure of 1.33 × 10^{-6} mbar · s. In line with the expectation from previous work [12,23], our STM images indicate that the OH$_b$ are replaced with a mixture of oxygen adatoms, surface hydroxyls, and O$_2$H species (i.e., O$_x$H$_y$ where $x = 1, 2$ and $y = 0, 1$) [12,23]. As shown by the data point denoted with a filled circle in Fig. 4(b), this exposure to O$_2$ also quenches the band-gap state, the peak only having 15% of its original intensity. Note that the UPS measurements are in this case performed at ~300 K in-
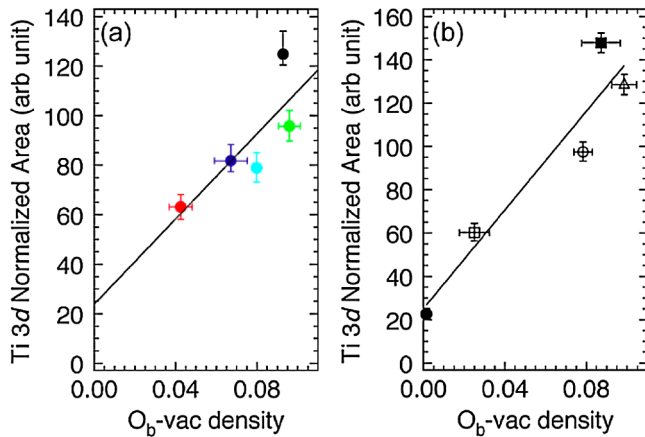
FIG. 4 (color online). Normalized integrated intensities of the band-gap state UPS peaks as a function of O_b vac density on the $TiO_2(110)$ surface determined from STM. The UPS spectra in the band-gap state region were fitted using the spectrum analysis software UNFIT 2004. In each case, the secondary electron background was fitted with a fourth-order polynomial while the band-gap state peak (located at ~0.9 eV below E_F) was fitted with a Gaussian function from which the normalized integrated intensity of the peak was extracted. (a) Data taken from experiments on as-prepared $TiO_2(110)$. The data points are color coded with the color borders in Figs. 2 and 3. (b) Data taken from experiments on hydroxylated $TiO_2(110)$ (in this case, the O_b vac density plotted is that before hydroxylation). The data points are from the initially hydroxylated surface (filled square), the oxidized surface (filled circle), and on the oxidized surface following electron bombardment for 2 (open square), 5 (open circle), and 10 s (open triangle). The black lines in both graphs represent the best linear fit.

stead of ~500 K to prevent the formation of TiO_x species on the oxygen-rich TiO_2 surface [14].

This oxidized surface (o-TiO_2) was subjected to electron bombardment for durations of 2, 5, and 10 s. The O_xH_y species are nearly all removed after electron bombardment for 2 s and are entirely removed after 5 s. More importantly, STM images show that the OH_b that were eliminated upon oxidation are replenished after electron bombardment (to be precise, electron bombardment leads to the formation of O_b vac, each of which is converted to two OH_b by exposure to water in the residual vacuum [10–12]). The density of OH_b created in this way increases with the duration of electron bombardment, as one would expect.

The graph in Fig. 4(b) shows that the band-gap state peak, which is quenched significantly by exposure to O_2, reappears and increases in intensity after electron bombardment (open square, open circle, and open triangle data points). This, together with the graph in Fig. 4(a), shows in

a very clear way that the population of the band-gap state depends directly on the concentration of O_b vac.

Examination of the graphs in Fig. 4, however, reveals that the population of the band-gap state does not depend *only* on the O_b vac density. The best-fit lines in both of the graphs in Fig. 4 do not pass through the origin. This indicates a small, but finite, band-gap state peak in UPS even when no O_b vac or OH_b are present. This means that although the major component to the band-gap state originates from O_b vac, there is a *minority* contribution that comes from some other defect, unconnected to O_b vac, such as interstitial Ti or subsurface oxygen vacancies.

In summary, we have used ultraviolet photoemission spectroscopy in combination with scanning tunneling microscopy to establish that the band-gap state in $TiO_2(110)$ originates mainly from bridging oxygen vacancies. Our results also show that the population of the band-gap state increases in direct proportion with the density of O_b vac. This is in direct contrast to a recent study which proposed that interstitial Ti make the dominant contribution to the band-gap state [14].

[1] *Metal Oxide Catalysis*, edited by S. D. Jackson and J. S. J. Hargreaves (Wiley-VCH, Weinheim, 2008).
[2] U. Diebold, Surf. Sci. Rep. **48**, 53 (2003).
[3] C. L. Pang, R. Lindsay, and G. Thornton, Chem. Soc. Rev. **37**, 2328 (2008).
[4] M. A. Henderson, Langmuir **12**, 5093 (1996).
[5] M. A. Henderson, Surf. Sci. **419**, 174 (1999).
[6] V. E. Henrich, G. Dresselhaus, and H. J. Zeiger, Phys. Rev. Lett. **36**, 1335 (1976).
[7] R. L. Kurtz et al., Surf. Sci. **218**, 178 (1989).
[8] W. S. Epling et al., Surf. Sci. **412–413**, 333 (1998).
[9] Z. M. Zhang, S. P. Jeng, and V. E. Henrich, Phys. Rev. B **43**, 12004 (1991).
[10] Z. Zhang et al., J. Phys. Chem. B **110**, 21840 (2006).
[11] O. Bikondoa et al., Nature Mater. **5**, 189 (2006).
[12] S. Wendt et al., Surf. Sci. **598**, 226 (2005).
[13] M. A. Henderson et al., J. Phys. Chem. B **107**, 534 (2003).
[14] S. Wendt et al., Science **320**, 1755 (2008).
[15] C. Di Valentin, G. Pacchioni, and A. Selloni, Phys. Rev. Lett. **97**, 166803 (2006).
[16] B. J. Morgan and G. W. Watson, Surf. Sci. **601**, 5034 (2007).
[17] C. J. Calzado, N. C. Hernández, and J. F. Sanz, Phys. Rev. B **77**, 045118 (2008).
[18] E. Finazzi, C. Di Valentin, and G. Pacchioni, J. Phys. Chem. C **113**, 3382 (2009).
[19] C. L. Pang et al., Nanotechnology **17**, 5397 (2006).
[20] N. G. Petrik et al., J. Phys. Chem. C **113**, 12407 (2009).
[21] M. Li et al., J. Phys. Chem. B **104**, 4944 (2000).
[22] T. Minato et al., Surf. Sci. **566–568**, 1012 (2004).
[23] Y. Du et al., J. Phys. Chem. C **113**, 666 (2009).